Chapter 64
Characterizing Fluctuations of Arterial and Cerebral Tissue Oxygenation in Preterm Neonates by Means of Data Analysis Techniques for Nonlinear Dynamical Systems

Stefan Kleiser, Marcin Pastewski, Tharindi Hapuarachchi, Cornelia Hagmann, Jean-Claude Fauchère, Ilias Tachtsidis, Martin Wolf, and Felix Scholkmann

Abstract The cerebral autoregulatory state as well as fluctuations in arterial (SpO_2) and cerebral tissue oxygen saturation (StO_2) are potentially new relevant clinical parameters in preterm neonates. The aim of the present study was to test the investigative capabilities of data analysis techniques for nonlinear dynamical systems, looking at fluctuations and their interdependence. StO_2, SpO_2 and the heart rate (HR) were measured on four preterm neonates for several hours. The fractional tissue oxygenation extraction (FTOE) was calculated. To characterize the fluctuations in StO_2, SpO_2, FTOE and HR, two methods were employed: (1) phase-space modeling and application of the recurrence quantification analysis (RQA), and (2) maximum entropy spectral analysis (MESA). The correlation between StO_2 and SpO_2 as well as FTOE and HR was quantified by (1) nonparametric nonlinear regression based on the alternating conditional expectation (ACE) algorithm, and (2) the maximal information-based nonparametric exploration (MINE) technique. We found that (1) each neonate showed individual characteristics, (2) a ~60 min oscillation was observed in all of the signals, (3) the nonlinear correlation strength between StO_2 and SpO_2 as well as FTOE and HR was specific for each neonate and showed a high value for a neonate with a reduced health status, possibly indicating an impaired cerebral

S. Kleiser • M. Pastewski • M. Wolf • F. Scholkmann (✉)
Biomedical Optics Research Laboratory, Department of Neonatology, University Hospital Zurich, University of Zurich, 8091 Zurich, Switzerland
e-mail: Felix.Scholkmann@usz.ch

T. Hapuarachchi • I. Tachtsidis
Department of Medical Physics and Bioengineering, University College London, London, UK

C. Hagmann • J.-C. Fauchère
Division of Neonatology, University of Zurich, 8091 Zurich, Switzerland

511

autoregulation. In conclusion, our data analysis framework enabled novel insights into the characteristics of hemodynamic and oxygenation changes in preterm infants. To the best of our knowledge, this is the first application of RQA, MESA, ACE and MINE to human StO_2 data measured with near-infrared spectroscopy (NIRS).

Keywords Long term measurements • Autoregulation • Near infrared spectroscopy • Correlation analysis • Spontaneous fluctuations

1 Introduction

Preterm infants exhibit an immature regulation of respiration as well as systemic and cerebral blood circulation (i.e. cerebral autoregulation, CO_2 vasoreactivity), leading to an increased incidence of hypoxic and hyperoxic episodes due to (1) large fluctuations in cerebral hemodynamics, and (2) impaired coupling between cerebral blood flow (CBF) and metabolic demand [1]. Episodes of intermittent hypoxemia occur in 74 % of preterm infants, compared to 62 % of term infants [2]. Hyperoxemia or hypoxemia may lead to an increase in mortality and neurological morbidity with long-term effects in later adult life. Greater variability in arterial oxygen saturation (SpO_2) [3] correlates with an increased incidence of retinopathy of prematurity (ROP). Thus, the assessment of the dynamics of SpO_2 and cerebral tissue oxygen saturation (StO_2) in preterm neonates may be of high clinical relevance. Due to continuous advancement in biomedical optics [4, 5], a reliable noninvasive long-term measurement of StO_2 in preterm neonates is in principle feasible [6, 7].

The aim of the present study was to analyze long-term measurements of StO_2 (conducted by multi-distance near-infrared spectroscopy, MD-NIRS) and SpO_2, heart rate (HR) and the fractional tissue extraction (FTOE) in preterm infants by means of data analysis techniques for nonlinear dynamical systems in order to investigate the characteristics of cerebral and systemic hemodynamic fluctuations and their interdependence.

2 Material and Methods

2.1 Subjects, Instrumentation and Experimental Protocol

A total of 20 clinically stable preterm neonates were enrolled. The study was approved by the ethics committee, and written informed consent was obtained from the parents before the study. Four neonates were selected for the present analysis, namely those with long continuous signals and the highest signal-to-noise ratio (SNR) (Table 64.1). SpO_2 and HR were determined by a standard patient monitor (Infinity Delta XL, Dräger, Germany) and StO_2 by an internally developed MD-NIRS device (OxyPrem, 4×3 [760, 805, 870 nm] light sources, two source-detector distances, i.e. 1.5, 2.5 cm [8]). OxyPrem uses the self-calibrating approach

Table 64.1 Description of the study sample

Characteristics	Neonate #1	Neonate #2	Neonate #3	Neonate #4
GA at birth (weeks)	33.4	26.4	29.4	26.8
GA at measurement (weeks)	34.7	28.5	29.9	30.7
Weight at measurement (g)	2220	1280	1090	1440
Apgar (1, 5, 10)	8, 8, 9	5, 4, 5	8, 8, 8	5, 8, 8
Respiration	Spontaneous	SIMV	CPAP	Spontaneous
FiO_2 (%), Hct (%), Hb (g/dL)	21, 50.6, 16.6	25, 40.9, 13.4	21, 49.5, 16.1	21, 36, 11.7
PDA	No	No	Yes	No
Length of analyzed data (min)	111	271	145	308

GA gestational age, *FiO_2* fraction of inspired oxygen, *SIMV* synchronized intermittent mandatory ventilation, *CPAP* continuous positive airway pressure, *Hct* hematocrit, *Hb* hemoglobin, *PDA* persistent ductus arteriosus

[9] which ensures a robust and high-precision measurement of absolute StO_2 values [10]. The NIRS optode was positioned over the left prefrontal cortex (PFC).

Measurements were performed continuously during the night (from ~10 pm till ~6 am), i.e. NIRS measured the resting-state activity of cerebral hemodynamics.

2.2   Signal Processing and Data Analysis

From the SpO_2 and StO_2 we calculated the fractional tissue oxygenation extraction (FTOE = (SpO_2-StO_2)/SpO_2) × 100 [%]. FTOE quantifies the balance between oxygen delivery and oxygen consumption and correlates significantly with the invasively measured oxygen extraction fraction [11]. All signals (SpO_2, StO_2, FTOE and HR) were downsampled to 0.05 Hz to increase the SNR and since only low frequencies were of interest. For each of the four datasets, an interval was chosen for the subsequent analysis which contains data without any signal distortion. The lengths of the data are given in Table 64.1. To characterize the fluctuations in StO_2, SpO_2, FTOE and HR, two different methods were applied:

- *Phase-space modeling and application of the recurrence quantification analysis* (*RQA*) [12, 13]. Each signal (StO_2, SpO_2, FTOE and HR) was embedded into a phase space with the dimension m and time delay τ. The optimal values for m and τ were determined by finding the first minimum of the false nearest neighbors function depending on m, and the autocorrelation function depending on τ, respectively. In a subsequent step, the phase space trajectories were characterized by the RQA. In particular, the determinism (*DET*, i.e. the predictability of the system), entropy of the diagonal length (*ENT*, i.e. the complexity of the system's deterministic dynamics), and laminarity (*LAM*, i.e. the amount of intermittency of the system's dynamics) were calculated.
- *Maximum entropy spectral analysis* (*MESA*) [14]. This method enables a high-precision spectral analysis based on the principle of maximum entropy.

To prevent spurious peaks, the order of the MESA-based periodogram was set at one third of the number of samples [15].

The correlation between StO_2 and SpO_2 as well as FTOE and HR were quantified by two nonparametric methods:

- *Nonparametric nonlinear regression based on the alternating conditional expectation* (*ACE*) *algorithm* [16]. This technique finds the optimal transformations for the dependent and independent variables in order to maximize the correlation. The correlation strength is quantified by the maximal correlation coefficient, r_{ACE}.
- *Maximal information-based nonparametric exploration* (*MINE*) *technique* [17]. MINE enables the characterization of dependencies between variables. We calculated the maximal information coefficient (*MIC*) (relationship strength) and maximum asymmetry score (*MAS*) (departure from monotonicity).

In addition, each signal was characterized by calculating the median, and variability index 1 (VI_1, quantified as the mean of the modulus of the first derivation). In addition, the relationship of the fluctuation strength of StO_2 vs. SpO_2 was determined by the ratio of their standard deviations (variability index 2, VI_2).

3 Results, Discussion, Conclusion and Outlook

Figure 64.1a–d shows the time courses of SpO_2, StO_2, HR and FTOE. In Fig. 64.1b the normalized (i.e. subtraction of the mean value) SpO_2 and StO_2 were plotted to increase the visibility of similar dynamics. Figure 64.1d shows FTOE and HR after normalization (z-score) and smoothing (Kolmogorov-Zurbenko filter, window length: 180 s, iterations: 2) which increases the visibility of the similar long-term variability of both signals. The ACE correlation plots as well as the RQA, ACE and MINE results are visualized in Fig. 64.2. All signals show subject-specific dynamics:

- RQA: Noticeable low values for *DET* and *LAM* in neonate #4, high values for neonate #1. *ENT* (for StO_2 and SpO_2) has low values for neonate #3.
- MESA: (1) Neonate #1 exhibited a large oscillation with a period length (T) of 60 min in StO_2 and SpO_2 as well as HR and FTOE. (2) A large oscillation with $T \approx 30$ min is present in neonate #2 for StO_2 and SpO_2, followed by a second strongest oscillation with $T \approx 60$ min. In FTOE the predominant oscillation was at $T \approx 60$ min. The spectra of StO_2 and SpO_2 have a remarkably similar fine structure of oscillatory peaks indicating a large degree of similarity in the dynamics. In addition, an oscillation with $T \approx 15$ min can be seen in StO_2, SpO_2, HR and FTOE. (3) Neonate #3 shows an oscillation peak with $T \approx 60$ min in StO_2, SpO_2, HR and FTOE, whereas for FTOE a larger oscillation with $T \approx 30$ min is present. The spectra of StO_2 and SpO_2 have different fine
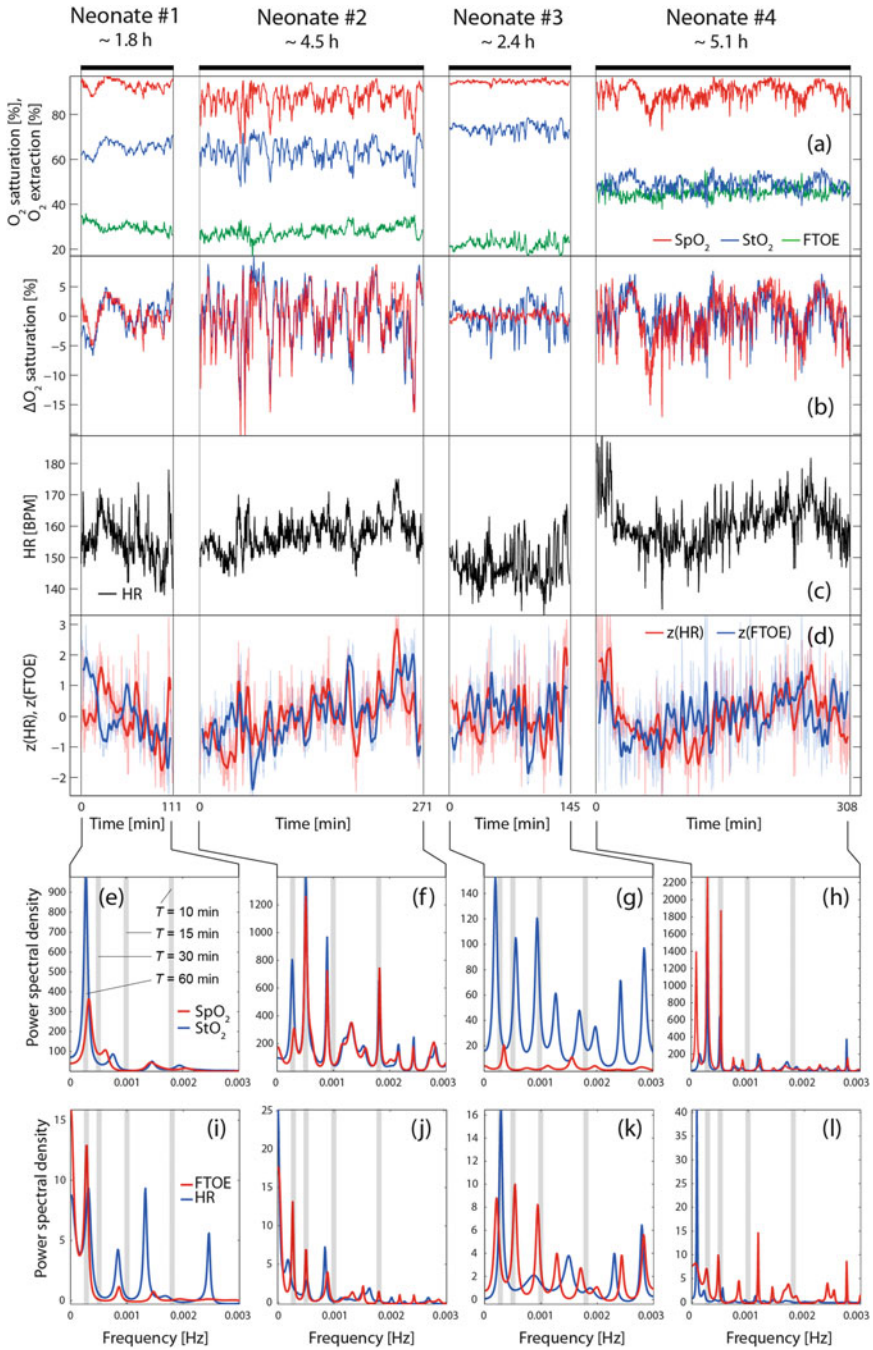
Fig. 64.1 (**a–d**) Visualization of the analyzed signals (StO_2, SpO_2, FTOE and HR). (**e–l**) Frequency spectra obtained by MESA
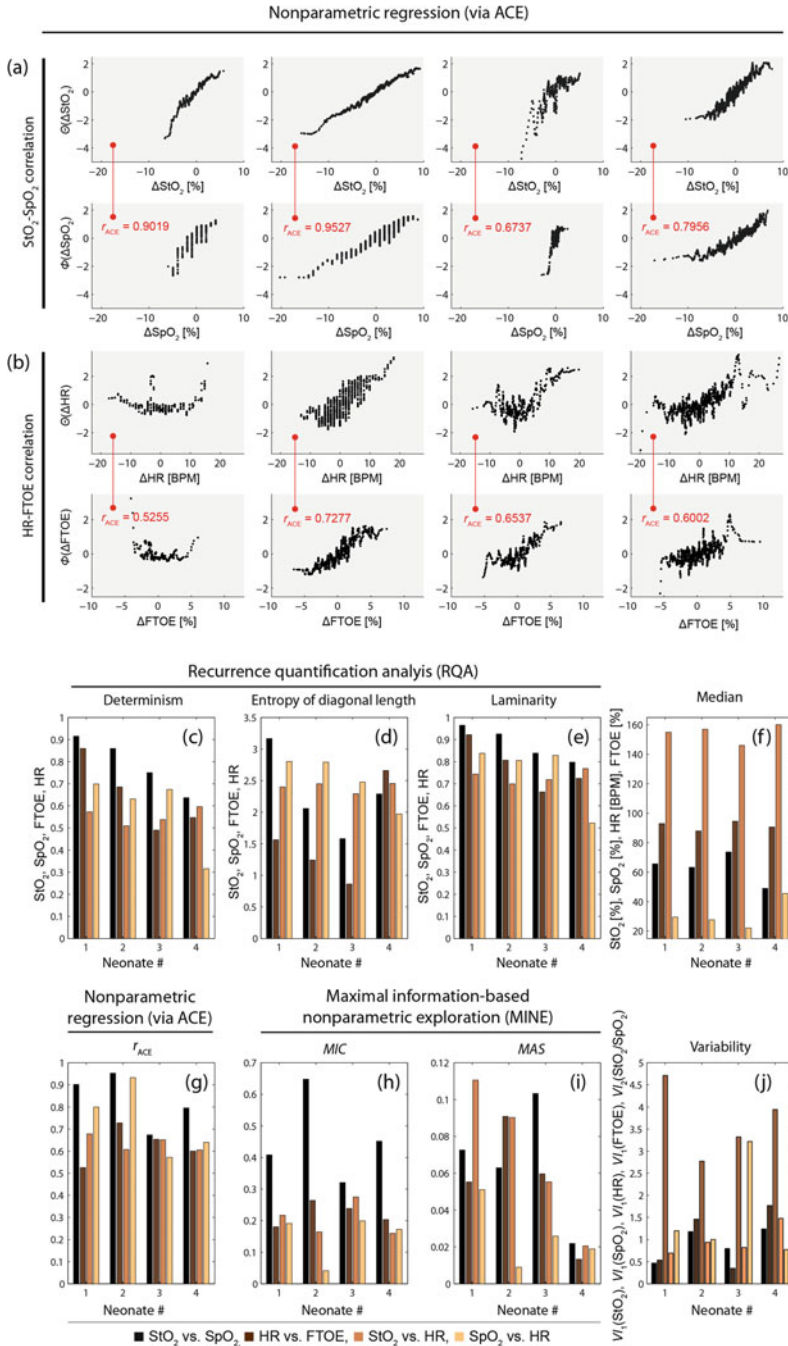
Fig. 64.2 (**a**, **b**) Correlation diagrams based on ACE nonparametric nonlinear regression. (**c–j**) Parameters obtained by RQA, MESA, ACE, MINE as well as the values for the median and variability

structures, which is also true for the spectra of HR and FTOE. (4) Neonate #4 shows a strong peak with $T \approx 60$ and 30 min in StO_2 and SpO_2.

- ACE and MINE: Concerning the relationship between StO_2 and SpO_2, the largest r_{ACE} and MIC value was found for neonate #2, the lowest for neonate #3; MAS was highest in neonate #3. Concerning HR vs. FTOE, neonate #2 had the largest r_{ACE}, MIC and MAS values. Neonate #4 showed significantly low MAS values for all four conditions (StO_2 vs. SpO_2 or HR, HR vs. FTOE or SpO_2).

To interpret the results it is helpful to discuss the similarities and differences of the signal characteristics with respects to the four neonates:

- *Similarities*: (1) The values for *DET*, *ENT* and *LAM* were all higher for StO_2 compared to SpO_2 (except for *ENT* of neonate #4), indicating more complex signal characteristics of StO_2 than of SpO_2. (2) The correlation between StO_2 and SpO_2 is higher than that observed between HR and FTOE ($r_{ACE}(StO_2, SpO_2) = 0.8310 \pm 0.1236$, $MIC(StO_2, SpO_2) = 0.4570 \pm 0.1385$; $r_{ACE}(HR, FTOE) = 0.6268 \pm 0.0854$, $MIC(HR, FTOE) = 0.2216 \pm 0.0371$). (3) All neonates showed an oscillation in StO_2, SpO_2, FTOE and HR with a period of $T \approx 60$ min, whereas the amplitude was specific for each neonate.
- *Differences*: (1) *DET*, *LAM* and *ENT* of SpO_2 were highest for neonate #3. (2) The correlation (r_{ACE}, MIC) between StO_2 and SpO_2 as well as HR and FTOE was highest for neonate #2; neonate #3 showed the lowest StO_2/SpO_2 correlation. (3) The smallest MAS values for all four correlations were found for neonate #4 (except for StO_2 vs. HR, neonate #2). (4) In neonate #3 we observed the highest median values for StO_2 and SpO_2 as well as the lowest ones for HR and FTOE. In neonate #4 the lowest StO_2 and the highest FTOE value were measured. (5) High VI_1 values in StO_2 and SpO_2 were present in neonates #2 and #4. Neonate #3 showed the largest VI_2 value for StO_2/SpO_2. (6) The mean StO_2 values correlated inversely with the individual Hct and GA (at birth) ($r = -0.927$ and $r = -0.982$, respectively; $p < 0.05$).

The physiological interpretation of these findings is not straightforward since all patient-specific characteristics have an influence on the analyzed parameters. In particular, the general health state (e.g. PDA, microbleeds, ischemia: yes/no), the type of respiration (ventilatory support: yes/no, type of support), and the GA (at birth/measurement) could potentially have a strong impact on the parameters. The following observations were made based on our analysis: (1) The general inverse correlation observed between StO_2 and Hct was also noticed by other studies (e.g. [18]). (2) Neonate #3 exhibited a large VI_2, e.g. the fluctuations in StO_2 were much stronger than in SpO_2 (especially the decreases), a pattern that is observed by neonates with a PDA—indeed, neonate #3 had a PDA (which was however classified as not hemodynamically relevant). The low StO_2/SpO_2 correlation (r_{ACE}, MIC) and the different frequency spectra (StO_2 vs. SpO_2, HR vs. FTOE) point also to a specific state of the systemic-cerebral hemodynamic coupling. The observation that neonate #3 had the highest median values for StO_2 and SpO_2 as

well as the lowest ones for HR and FTOE is surprising since one would expect an increased FTOE and decrease StO_2 in case of a PDA [19]. (3) The oscillations in the data with $T \approx 60$ and 30 min could originate from sleep phases. A sleep-wake cycling (with a quiet sleep phase with $T \approx 20$ min) is known [20] in term newborns with $T \approx 50$–60 min and an increase in total hemoglobin and HR during active sleep (compared to quite sleep) has previously been observed [21, 22]. (4) The two neonates with the lowest GA at birth (#2, #4) had the largest variability of StO_2, SpO_2 and FTOE which could indicate an immature functioning of cerebral hemodynamic regulation.

In conclusion, using four case studies, we demonstrated the possibility of realizing long-term measurements in preterm neonates with MD-NIRS and we presented a novel framework for investigating the characteristics of cerebral and systemic hemodynamic fluctuations and their interdependence. A follow-up study, investigating the signal characteristics in healthy and ill preterm neonates using the same framework would be the next step. Focusing on the fluctuation characteristics of the signals may offer novel insights into systemic and cerebral hemodynamics that are not assessed routinely only using traditional analyses (i.e. based on moments and linear correlations). To the best of our knowledge, this is the first application of RQA, MESA, ACE and MINE to human NIRS data.

References

1. Fyfe KL et al (2013) The development of cardiovascular and cerebral vascular control in preterm infants. Sleep Med Rev 18:299–310
2. Hunt CE et al (2011) Longitudinal assessment of hemoglobin oxygen saturation in preterm and term infants in the first six months of life. J Pediatr 159(3):377–383
3. Di Fiore JM et al (2012) The relationship between patterns of intermittent hypoxia and retinopathy of prematurity in preterm infants. Pediatr Res 72(6):606–612
4. Scholkmann F et al (2014) A review on continuous wave functional near-infrared spectroscopy and imaging instrumentation and methodology. Neuroimage 85(Part 1):6–27
5. Wolf M, Ferrari M, Quaresima V (2007) Progress of near-infrared spectroscopy and topography for brain and muscle clinical applications. J Biomed Opt 12(6):062104
6. Wolf M, Greisen G (2009) Advances in near-infrared spectroscopy to study the brain of the preterm and term neonate. Clin Perinatol 36(4):807–834
7. Wolf M et al (2012) A review of near infrared spectroscopy for term and preterm newborns. J Near Infrared Spectrosc 20(1):43–55
8. Hyttel-Sorensen S et al (2013) Calibration of a prototype NIRS oximeter against two commercial devices on a blood-lipid phantom. Biomed Opt Express 4(9):1662–1672
9. Hueber DM et al (1999) New optical probe designs for absolute (self-calibrating) NIR tissue hemoglobin measurements. Opt Tomogr Spectrosc Tissue III Proc SPIE 3597:618–631

10. Scholkmann F, Metz AJ, Wolf M (2014) Measuring tissue hemodynamics and oxygenation by continuous-wave functional near-infrared spectroscopy – how robust are the different calculation methods against movement artifacts? Physiol Meas 35(4):717–734
11. Naulaers G et al (2007) Use of tissue oxygenation index and fractional tissue oxygen extraction as non-invasive parameters for cerebral oxygenation. A validation study in piglets. Neonatology 92(2):120–126
12. Webber CL Jr, Zbilut JP (1985) Dynamical assessment of physiological systems and states using recurrence plot strategies. J Appl Physiol 76(2):965–973
13. Marwan N et al (2002) Recurrence plot based measures of complexity and its application to heart rate variability data. Phys Rev E 66(2):026702
14. Ulrych TJ, Bishop TN (1975) Maximum entropy spectral analysis and autoregressive decomposition. Rev Geophys 13(1):183–200
15. Kay SM (1979) The effects of noise on the autoregressive spectral estimator. IEEE Trans Acoust Speech Signal Process 27(5):478–485
16. Breiman L, Friedman JH (1985) Estimating optimal transformations for multiple regression and correlation. J Am Stat Assoc 80(391):580–598
17. Reshef DN et al (2011) Detecting novel associations in large data sets. Science 334 (6062):1518–1524
18. Youkin DP et al (1987) The effect of hematocrit and systolic blood pressure on cerebral blood flow in newborn infants. J Cereb Blood Flow Metab 7(3):295–299
19. Vanderhaegen J et al (2008) Surgical closure of the patent ductus arteriosus and its effect on the cerebral tissue oxygenation. Acta Paediatr 97(12):1640–1644
20. Osredkar D et al (2005) Sleep-wake cycling on amplitude-integrated electroencephalography in term newborns with hypoxic-ischemic encephalopathy. Pediatrics 115(2):327–332
21. Münger DM, Bucher HU, Duc G (1998) Sleep state changes associated with cerebral blood volume changes in healthy term newborn infants. Early Hum Dev 52(1):27–42
22. Stéphan-Blanchard E et al (2013) Heart rate variability in sleeping preterm neonates exposed to cool and warm thermal conditions. PLoS One 8(7):e68211